Cholesterol Hydroxyl Group Is Found To Reside in the Center of a Polyunsaturated Lipid Membrane

Thad A. Harroun,[‡,§] John Katsaras,[‡,⊥] and Stephen R. Wassall*[,∥]

National Research Council, Canadian Neutron Beam Centre, Chalk River, Ontario K0J 1J0, Canada, Guelph-Waterloo Physics Institute and Biophysics Interdepartmental Group, University of Guelph, Guelph, Ontario N1G 2W1, Canda, Department of Physics, University of Guelph, Guelph, Ontario N1G 2W1, Canada, and Department of Physics, Indiana University−Purdue University Indianapolis, Indianapolis, Indiana 46202-3273

Received October 12, 2005; Revised Manuscript Received November 29, 2005

ABSTRACT: Cholesterol and saturated lipid species preferentially partition into liquid ordered microdomains, such as lipid rafts, away from unsaturated lipid species for which the sterol has less affinity in the surrounding liquid-disordered membrane. To observe how cholesterol interacts with unsaturated phospholipids, we have determined, from one-dimensional neutron scattering length density profiles, the depth of cholesterol in phosphatidylcholine (PC) bilayers with varying amounts of acyl chain unsaturation. Through the use of [2,2,3,4,4,6-$^2H_6$]-labeled cholesterol, we show that in 1-palmitoyl-2-oleoylphosphatidylcholine (16:0−18:1 PC), 1,2-dioleoylphosphatidylcholine (18:1−18:1 PC), and 1-stearoyl-2-arachidonylphosphatidylcholine (18:0−20:4 PC) bilayers the center of mass of the deuterated sites is approximately 16 Å from the bilayer center. This location places the hydroxyl group of the sterol moiety at the hydrophobic/hydrophilic bilayer interface, which is the generally accepted position. In dramatic contrast, for 20:4−20:4 PC membranes the hydroxyl group is found, unequivocally, sequestered in the bilayer center. We attribute the change in location to the high disorder of polyunsaturated fatty acids (PUFA) that is incompatible with close proximity to the steroid moiety in its usual "upright" orientation.

The physiological importance of (PUFA)[1] is becoming increasingly evident (*1*). High concentrations of PUFA-containing phospholipids are found in neural membranes, where they are essential for neurological function, and many health benefits are derived from dietary food sources rich in PUFA, whose lipids are eventually incorporated into the phospholipids of plasma membranes. It has been hypothesized that the poor affinity of cholesterol, which is abundant in the plasma membrane of most animal cells, for PUFA-containing phospholipids plays a crucial biological role (*2*−*4*). According to this hypothesis, the low mutual affinity drives the formation of polyunsaturated lipid-rich/sterol-poor microdomains and saturated lipid-rich/sterol-rich microdomains, such as lipid rafts, that provide the necessary local environment for protein function. Here, the previously unexplored effect of polyunsaturation upon the depth to which cholesterol penetrates the membrane is investigated by means of neutron scattering.

A primary role of cholesterol is to modulate molecular organization within membranes (*5*). Its interaction with saturated fatty acid (SFA)-containing phosphatidylcholines (PC) is well-characterized. The introduction of the rigid steroid moiety into homoacid-disaturated PC membranes disrupts the regular packing of chains in the gel or solid-ordered (so) phase and restricts the reorientation of the fatty acid chains in the liquid crystalline or liquid-disordered (ld) phase (*6*). The differential between the phases is smeared out until a liquid-ordered (lo) phase, characterized by rapid reorientation but high conformational order, is formed over a wide range of temperatures at concentrations >25 mol %. Excess sterol is expelled when the content exceeds >50 mol % (*7*). Within the membrane, the 3β-hydroxyl group of cholesterol locates just below the aqueous interface (*8*) and the steroid moiety rotates rapidly about the long molecular axis that wobbles through a narrow range of angles slightly tilted relative to the bilayer normal (*9*). A similar behavior is exhibited by heteroacid-saturated−monounsaturated PC (*10*−*12*).

The interaction of cholesterol with polyunsaturated fatty acid (PUFA)-containing phospholipids is much less understood and has only recently begun to receive attention. A variety of biophysical measurements have revealed that the sterol has an aversion to PUFA (*2*, *3*, *13*, *14*). The tremendous reduction in the amount of cholesterol that dipolyunsaturated PC membranes can accommodate points to this reduced affinity. Specifically, a solubility limit of ≤15 mol % was measured in 1,2-diarachidonylphosphatidylcholine (20:4−20:4 PC) (*15*) and 1,2-didocosahexaenoylphosphatidylcholine (22:6−22:6 PC) (*16*) by X-ray diffraction and solid-state ^2H NMR. This poor affinity of cholesterol for PUFA-containing PC has been attributed to the high conformational disorder of the PUFA chains, the result of a

* To whom correspondence should be addressed: Department of Physics, Indiana University−Purdue University Indianapolis, Indianapolis, IN 46202-3273. Telephone: 317-274-6908. Fax: 317-274-2393. E-mail: swassall@iupui.edu.

‡ Canadian Neutron Beam Centre.

§ Department of Physics, University of Guelph.

⊥ Guelph-Waterloo Physics Institute and Biophysics Interdepartmental Group, University of Guelph.

∥ Indiana University−Purdue University Indianapolis.

[1] Abbreviations: PC, phosphatidylcholine; PUFA, polyunsaturated fatty acids; SFA, saturated fatty acids.

10.1021/bi0520840 CCC: $33.50
Published on Web 01/10/2006

low energy barrier to rotation about the single bonds that separate the multiple double bonds in the recurring ═C−C−C═ motif (*17*). Whereas a SFA chain adopts an all-trans configuration, presenting a smooth facade and facilitating intimate contact with the rigid steroid moiety, a highly dynamic and disordered PUFA chain deters such proximity with cholesterol. The current study employs neutron scattering to determine how this unfavorable interaction with PUFA affects the location of cholesterol within a membrane. A remarkable change in the depth to which the sterol penetrates a dipolyunsaturated phospholipid membrane is identified.

Neutron Diffraction and Deuterium Labeling. The success of neutron diffraction to locate individual membrane components along the normal of the bilayer plane is well-established. The technique relies on the specific deuterium labeling of molecular groups and the Fourier reconstruction of the bilayer profile from the diffraction data. The unique ability of neutrons to distinguish between hydrogen and deuterium atoms provides the signal from the deuterium label, which remains once all of the unlabeled sample data has been subtracted away.

One of the first demonstrations of the technique was provided by Zaccaï et al. (*18*), who identified the various molecular components of a 1,2-dipalmitoylphosphaitylcholine (16:0−16:0 PC) bilayer (*19*, *20*). Since then, the molecular components of bilayers formed, for example, from 1,2-dioleoylphosphatidylcholine (18:1−18:1 PC) (*21*, *22*) and phosphatidylinositol (*23*) lipids have been measured. The location of several membrane-bound molecules has also been determined. They include anaesthetics (*2*), squalene (*25*), selectively labeled protein residues (*26*, *27*), and cholesterol in homoacid-disaturated and heteroacid-saturated−monounsaturated PC bilayers (*8*, *11*).

Structure determination of lipid bilayers is complicated by the disorder present within the bilayers, because of the high mobility of molecules in all directions as well as vibrations and undulations of the membrane itself. Consequently, the measured structural profile of the bilayer in the direction normal to the plane of the bilayer, be it from X-rays (electron density) or neutrons (scattering length density, SLD), is inherently of lower resolution. Higher resolution profiles can be gained through partial dehydration and alignment of the bilayers on a flat substrate. However, the commonly defined resolution, d/h_{max}, remains on the order of 6−11 Å. Here, d is the unit-cell size or the repeat distance of the multilamellar stack, and h_{max} is the number of measured quasi-Bragg diffraction orders.

On the other hand, the accuracy of the location and distribution of a specific deuterium label is quite high. Gordeliy and Chernov (*28*) have theoretically demonstrated that, with only 4 diffraction orders, the label position can be determined with an accuracy of better than 1 Å and the width of the distribution of a label to an accuracy of better than ∼5%. What this means is that the measured label distributions are suitable for a direct comparison with those obtained from theroetical molecular models.

In this paper, we report the location of the hydroxyl end of the cholesterol steroid in membranes with varying degrees of acyl chain unsaturation. In bilayers composed of PC molecules with a saturated acyl chain at the *sn*-1 position or a monounsaturated acyl chain at both *sn*-1 and *sn*-2 positions, the "top" of the steroid moiety resides 16 ± 1 Å from the bilayer center. This value corresponds to the location previously measured for cholesterol (*8*). However, in a dipolyunsaturated PC bilayer, when the entire hydrocarbon matrix consists of PUFA chains, our measurements indicate that the "top" of the cholesterol steroid structure relocates to the center of the bilayer.

MATERIALS AND METHODS

Phosphorylcholine lipids were purchased from Avanti Polar Lipids (Alabaster, AL) and prior to use were tested for degradation with TLC. The lipids studied were of the form 1-acyl-2-acyl-*sn*-glycero-3-phosphorylcholine, where the acyl chains were either palmitoyl-oleoyl, (16:0−18:1 PC), di-oleoyl (18:1−18:1 PC), stearoyl-arachidonoyl (18:0−20:4 PC), or di-arachidonoyl (20:4−20:4 PC). Sigma (St. Louis, MO) and CDN Isotopes (Pointe-Claire, Québec, Canada) were, respectively, the source of unlabeled cholesterol and selectively deuterated [2,2,3,4,4,6-$^2H_6$] cholesterol.

All preparations of aligned multilayer samples were carried out in a helium-filled glovebox, and to ensure that the solubility limit was not exceeded in the case of the dipolyunsaturated PC, the amount of cholesterol was set at 10 mol %. Because PUFA-containing phospholipid samples are susceptible to peroxidation, they were checked for odor, which is a sensitive indicator of sample degradation, before and after data collection. Suspect samples were checked for purity by TLC and, if found to be degraded, were remade. A total of 12 mg of phospholipid and cholesterol was codissolved in chloroform−trifluoroethanol (3:1). The solution was then deposited on a silicon crystal substrate, and the solvent evaporated while gently rocking the sample. The sample was then placed in a vacuum for ∼2 h to remove traces of the solvent.

Neutron diffraction data were taken on the N5 beam-line at the Canadian Neutron Beam Center (Chalk River, Ontario, Canada), using 2.37 Å wavelength neutrons selected by the (002) reflection of a pyrolytic graphite (PG) monochromator, while a PG filter was used to eliminate higher order (i.e., $\lambda/2$, etc.) reflections. The samples were equilibrated in a humid, helium atmosphere at room temperature for several hours and kept at 24.0 ± 0.5 °C during data collection. Samples were hydrated at fixed humidities using saturated salt solutions of KCl (84% RH) and KNO_3 (94% RH) with 8 mol % ^2H_2O. Because of time constraints, only a few samples were measured at an additional ^2H_2O concentration of 20 mol %. These samples consistently reproduced the same d spacing as the 8 mol % ^2H_2O samples at the same relative humidty, which points to the reproducibility of the results.

Typically, $h_{max} = 5$ orders of Bragg diffraction was recorded as illustrated in Figure 1. The unit-cell size varied between 45 and 54 Å, meaning that the data have a commonly defined resolution of 9−11 Å. Linear backgrounds were subtracted from the signal, and the quasi-Bragg peaks were fit with Gaussians. The area of the peak is the measured integrated intensity, $I(q)$, as a function of the scattering vector, $q = 4\pi \sin(\theta)/\lambda$, where λ is the wavelength and θ is the scattering angle. The intensity was corrected using the following terms. First, in a narrow, Gaussian incident shaped beam, there is a varying neutron flux

Table 1: Tabulated Measured and Calculated Form Factors for Membranes that Contain the Deuterium-Labeled Cholesterol (Table D) and the Normal Cholesterol (Table H)[a]

Table D

	16:0−18:1 PC		18:1−18:1 PC		18:0−20:4 PC		20:4−20:4 PC	
	F^D	δF	F^D	δF	F^D	δF	F^D	δF
F_0	3.704		4.101		5.117		7.003	0.059
F_1	−2.487	0.056	−3.034	0.045	−1.688	0.026	−1.730	0.056
F_2	−1.100	0.056	−1.323	0.045	−0.989	0.026	−1.799	0.056
F_3	0.713	0.056	0.931	0.045	0.472	0.026	0.621	0.056
F_4	−0.278	0.057	−0.537	0.046	−0.224	0.026	−0.386	0.056
F_5	−0.129	0.058	−0.190	0.047	−0.053	0.026		

Table H

	16:0−18:1 PC		18:1−18:1 PC		18:0−20:4 PC		20:4−20:4 PC	
	F^H	δF	F^H	δF	F^H	δF	F^H	δF
F_0	3.088		3.503		4.535		6.775	
F_1	−2.241	0.012	−2.714	0.037	−1.479	0.031	−1.919	0.064
F_2	−0.648	0.012	−0.872	0.037	−0.574	0.031	−1.886	0.064
F_3	0.460	0.012	0.516	0.038	0.264	0.032	0.571	0.065
F_4	−0.266	0.012	−0.328	0.038	−0.154	0.032	−0.422	0.064
F_5	−0.049	0.012	−0.056	0.038				

[a] The values of F_0 were estimated on the basis of the chemical composition and a mass density of 1 g/cm^3. The errors of the form factors arise from fitting the measured values of F_h at different hydrations to a single form factor curve as described in the text.

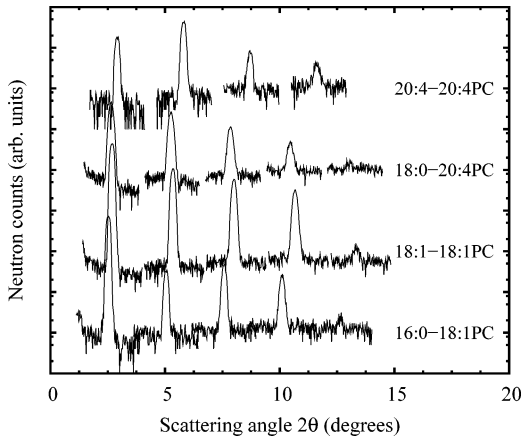

FIGURE 1: Example of raw diffraction data for each of the lipids studied. Note the increase in the second-order intensity around 5° for 20:4−20:4 PC compared to the other lipids, indicating an increase in the SLD in the center of the bilayer relative to the interbilayer water layer.

impinging on the sample as the sample angle is varied to cover the necessary q values. This correction is given by

$$C_{\text{flux}} = 1/\text{erf}\left(\frac{L\sin(\theta)}{\sqrt{8}\sigma}\right)$$

where erf is the error function, σ is the width of the beam, and L is the width of the sample. The Lorentz correction $C_{\text{Lor}} = \sin(2\theta)$ is then applied. Finally, the data are corrected for sample absorption in the following manner:

$$C_{\text{abs}} = \alpha/(1 - e^{-\alpha}), \qquad \alpha = \frac{2\mu t}{\sin(\theta)}$$

where μ is the calculated absorption coefficient and t is the sample thickness. The amplitude of the form factor for each quasi-Bragg reflection is then given by $|F(q)|^2 = C_{\text{flux}}C_{\text{Lor}}C_{\text{abs}}I$.

The SLD profile $\rho(z)$ was constructed as follows:

$$\rho(z) = F_0 + 2\sum_{h=1}^{h_{\max}} F_h \cos(2\pi z h/d)$$

where z is the distance along the bilayer normal and $z = 0$ is defined as the center of the bilayer. To put the data on an absolute scale, the forward scattering intensity, F_0, must be known. However, because it cannot be measured, it has to be estimated. We calculate these values based on the chemical composition and the assumption of a mass density of 1 g/cm^3. The values are listed in Table 1. Data were then placed on an absolute scale by requiring that the area in the difference SLD profile be equal to the scattering length of the label, of 6 deuterium minus 6 hydrogen.

The phases of the SLD Fourier reconstruction were determined by a method different from previous measurements (*11*, *19*). We take advantage of the fact that a mixture of 8 mol % ^2H_2O in H_2O has a net zero SLD; therefore, the scattering arises only from the lipid molecules, whose structure is assumed to change only slightly with changes in interbilayer water content for relative humidities between 80 and 95% (*29*). Because the only changing mass in the unit cell is from the water, the total SLD of the unit cell, that is $\rho_{\text{tot}} = \int_0^d \rho(z)dz = F_0$, does not change with differences in hydration. In other words, the form factor, i.e., the lipid bilayer, should not change with the swelling of the unit cell. The structure factor amplitudes can thus be plotted on a single form factor curve (*29*), which is not the case for bilayers such as, gel-phase 1,2-dimyristoylphosphatidylcholine (14:0−14:0 PC) and 16:0−16:0 PC whose chain tilt varies with hydration (*30*, *31*). In this manner, the correct form factor can be interpolated or extrapolated to a given d spacing. Moreover, it is then possible to match the d spacing between experiments more precisely.

RESULTS AND DISCUSSION

Figure 2 shows the SLD profiles of unlabeled cholesterol in 16:0−18:1 PC, 18:1−18:1 PC, 18:0−20:4 PC, and

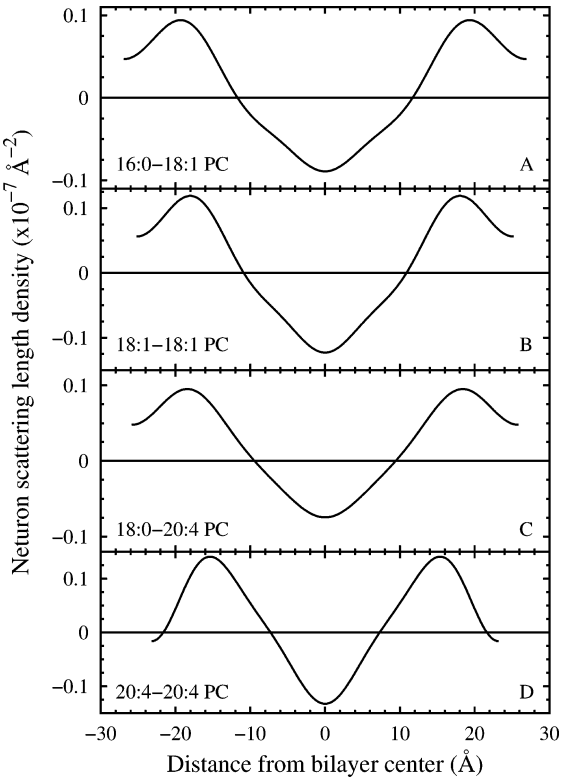

FIGURE 2: SLD of bilayers, including water, containing unlabeled cholesterol. The origin of the abscissa is the center of the bilayer. The calculated SLD profiles have a spatial resolution of ~10 Å and contain obvious features. The negative dip at the center is from the terminal methyls, and the broad, positive peaks are due to the glycerol−ester through phosphate regions. The bilayer thickness is defined as the distance between the maxima of the two peaks.

Table 2: Tabulated Data of the Measured and Calculated Structural Parameters[a]

lipid	repeat spacing (Å)	bilayer thickness (Å)	label depth (Å)	label width (Å)
16:0−18:1 PC	54.5	36.5	16.2 ± 0.5	5.8 ± 0.6
18:1−18:1 PC	52.0	34.7	16.4 ± 0.3	4.2 ± 0.2
18:0−20:4 PC	52.9	34.9	15.6 ± 0.4	5.9 ± 0.5
20:4−20:4 PC	46.4	30.6	0.0 ± 0.0	6.5 ± 0.3

[a] The bilayer thickness is defined as the peak−peak distance of the bilayer SLD profiles shown in Figure 2. The center and width of the label locations are determined from the Gaussian peak fits to the difference SLD profiles shown in Figure 3.

20:4−20:4 PC bilayers. The origin of the abscissa is the centrosymmetric center of the unit cell, which corresponds to the center of the bilayer, while the interlamellar water layer is at the edges of the unit cell. The maximum in the SLD corresponds to the combined glycerol−ester and phosphate regions of the lipid bilayer. Values for the putative bilayer hydrophobic thickness, defined by the distance between these peaks, are presented in Table 2. The negative dip in SLD, corresponding to the bilayer center, is due to the disordered terminal methyl groups of the acyl chains.

Inspection of the profiles for 16:0−18:1 PC (Figure 2A) and 18:1−18:1 PC (Figure 2B) reveals a small "kink" as one moves from the bilayer center toward the headgroups. This feature has previously been determined to correspond to the location of the double bond in oleoyl fatty acid chains (*21*, *22*). In 18:0−20:4 PC (Figure 2C) and 20:4−20:4 PC (Figure 2D), there is less evident structure in the acyl chain region of the SLD profile, resulting in a more "V"-like-shaped hydrophobic region that reflects the elevated conformational flexibility associated with the multiple double bonds in the arachidonyl chain. A similar profile was previously seen in the electron-density profile for 1-palmitoyl-2-arachidonoylphosphatidylcholine (16:0−20:4 PC) bilayers (*32*) and also for more highly unsaturated docosahexaenoyl-containing PC bilayers (*32*, *33*).

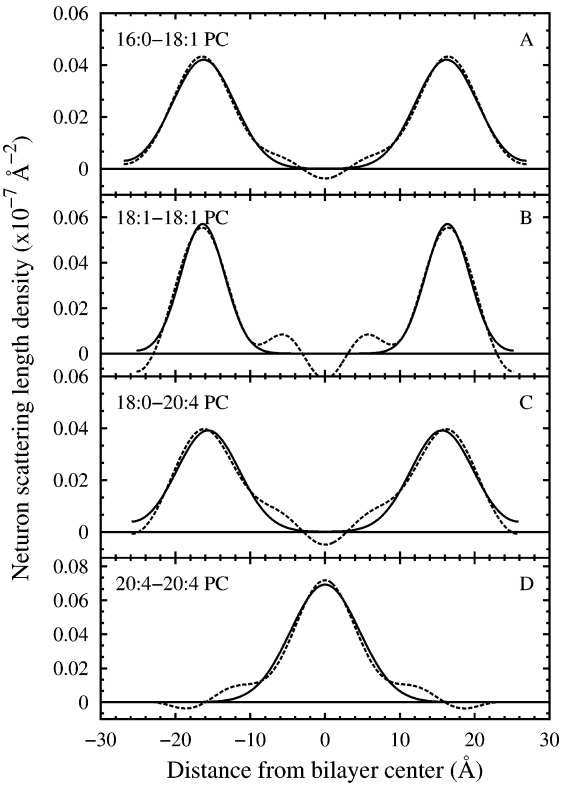

FIGURE 3: SLD difference profiles between labeled and unlabeled samples. The bilayer orientation is the same as in Figure 2. The dashed line is the measured data, and the solid line is a fit with a single Gaussian function. Fitting is performed in reciprocal space by taking the difference in the measured form factors.

Figure 3 shows the difference profiles between the deuterium-labeled and unlabeled cholesterol from Figure 2. The difference is dominated by a single pair of Gaussian-shaped peaks symmetrically disposed on either side of the origin (parts A−C of Figure 3) or a single Gaussian-shaped peak centered at the origin (Figure 3D) above a fluctuating background. These peaks designate where the center of mass of the six deuterated sites on the labeled sterol sits within each membrane. The solid line is a single Gaussian function fit to the difference data, which is used to determine the location and width. The fitted values are listed in Table 2. Moreover, the appearance of a single Gaussian is indicative of a single population for the label.

For 16:0−18:1 PC (Figure 3A), 18:1−18:1 PC (Figure 3B), and 18:0−20:4 PC (Figure 3C) the label appears approximately 16 Å from the bilayer center. This location coincides with that usually found for cholesterol in a membrane. It places the hydroxyl group of the sterol moiety, which is 1.9 Å away from the center of mass of the deuterons, within the hydrophobic/hydrophilic interfacial region (*8*). A schematic rendition is offered in Figure 4A. Although the bilayer thickness decreases by nearly 2 Å from

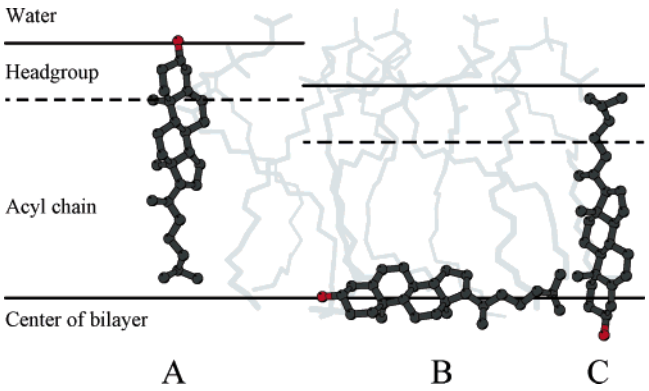

FIGURE 4: Schematic of the calculated locations and orientations of cholesterol in a membrane. A gray background of model phospholipids is shown for illustration purposes. (A) Canonical location and orientation of cholesterol in a bilayer. The "top" of the steroid ring is located 16 Å from the bilayer center, as measured in 16:0−18:1 PC, 18:1−18:1 PC, and 18:0−20:4 PC bilayers. (B and C) For 20:4−20:4 PC bilayers, the steroid label is at the center of the bilayer and shown here in two possible orientations; lying flat within the acyl chain matrix or inverted from its typical configuration. The bilayer thickness, indicated by the horizontal lines, is considerably less for the 20:4−20:4 PC bilayer. The figure was prepared with Molscript (*37*).

16:0−18:1 PC to 18:1−18:1 PC and 18:0−20:4 PC (Table 2), the cholesterol resides within ~0.5 Å, in approximately the same location in all three bilayers. When only the hydroxyl end is labeled, we cannot measure the degree of tilt that the sterol has in these PC bilayers. Solid-state ^{2}H NMR spectra for equimolar [3α-^{2}H$_1$]cholesterol incorporated into homoacid-disaturated (*34*) and heteroacid-saturated−unsaturated PC bilayers (*12*) indicate a most probable orientation (tilt angle) of $\alpha_0 = 16 \pm 1°$ relative to the bilayer normal for the long molecular axis, irrespective of the number of double bonds in the *sn*-2 chain. Figure 4A shows a generic picture of the orientation of cholesterol, with its long molecular axis toward the bilayer center. The sample- and time-averaged motion of cholesterol is measured in the width of the label peak (Table 2). These values range from 4.2 Å in 18:1−18:1 PC to 5.8 and 5.9 Å in 16:0−18:1 PC and 18:0−20:4 PC, respectively, and there seems to be no correlation associated with the degree of hydrocarbon chain unsaturation. Perhaps protruding almost 1 Å further into the membrane surface, as implied by our data for 18:1−18:1 PC (Table 2), restricts the transverse motion of cholesterol.

In marked contrast to 16:0−18:1 PC, 18:1−18:1 PC, and 18:0−20:4 PC, for 20:4−20:4 PC, the headgroup region of the bilayer SLD profile is unaltered in the presence of labeled cholesterol. However, after subtraction, the difference SLD displays excess SLD in the center of the bilayer, as shown in Figure 3D. The best fit to a single Gaussian requires that the label depth parameter be fixed at 0 Å, i.e., the bilayer center. This result clearly establishes that the cholesterol molecule has undergone a major reorientation within the dipolyunsaturated membrane, such that its hydroxyl group is now located in the middle of the bilayer. The question that this surprising observation raises is whether the sterol lies flat between monolayers or, less likely, has become inverted in the bilayer. These two options are illustrated in parts B and C of Figure 4, in conjunction with the much thinner 20:4−20:4 PC bilayer.

If we consider 16:0−18:1 PC, 18:1−18:1 PC, and 18:0−20:4 PC, the maxima associated with the glycerol−ester and phosphate peaks in the SLD profile (parts A−C of Figure 2) lie 1−2 Å outside the maxima for the cholesterol label peaks in the difference SLD profile (parts A−C of Figure 3). The transition between the hydrophobic membrane interior and hydrophilic aqueous environment will not be sudden but may be well-represented by this 1−2 Å region. Note that the thickness of the 20:4−20:4 PC bilayer is >4 Å less than in the other cases, which is reflected in Figure 4. The peak of the glycerol−ester and phosphate region is now at 15 Å, below the depth that would be occupied by the hydroxyl end of cholesterol in its "usual" position. Simply, there is not enough room for the sterol molecule to stand upright within the 20:4−20:4 PC membrane without protruding into the opposite leaflet, which may be a key factor in promoting a change in orientation. The thinness of the dipolyunsaturated bilayer, together with the related large cross-sectional molecular area (*35*), originates in the extremely high disorder that rapid interconversion between torsional states in polyunsaturated chains produces. An increased volume density of acyl chains toward the membrane surface of the type identified for PUFA chains by MD simulations (*33*) would further tend to favor placing the bulky steroid moiety in the center of the membrane. Once there, it is conceivable that the −OH groups of cholesterol might join to form dimers that further anchor that part of the molecule in the bilayer center. Such an arrangement could apply to sterols from opposing leaflets in an inverted orientation or to sterols aligned parallel to the plane of the bilayer.

We speculated on the possibility that cholesterol penetrates deeply into the hydrophobic core of the 20:4−20:4 PC membrane in a previous study (*15*). The rationale came from the poor affinity of cholesterol for polyunsaturated versus saturated chains evidenced by solid-state ^{2}H NMR and X-ray diffraction measurements of a dramatic reduction in the solubility for the sterol in 20:4−20:4 PC. Whereas PCs possessing a saturated *sn*-1 chain can accommodate >50 mol % cholesterol independent of the degree of unsaturation in the *sn*-2 chain, the solubility in 20:4−20:4 PC when there must be close contact with polyunsaturated chains is limited to 15 mol %. We therefore reasoned that locating the sterol in the middle of the dipolyunsaturated bilayer would alter two important interactions. First, it would minimize the proximity to the sequence of methylene-interrupted double bonds that runs from C5 to C15. Second, it would maximize the proximity to the 5 single bonds that runs from C15 to C20 at the terminal methyl end of arachidonyl chains. The findings reported here, as discussed above, offer a refinement of this proposal.

Consistent with a profound difference in molecular organization, the order parameter S_{CD} determined from ^{2}H NMR spectra observed for [3α-^{2}H$_1$]cholesterol added to multilamellar dispersions in our earlier work is also substantially smaller for 20:4−20:4 PC ($S_{CD} = 0.29$) than PCs comprised of a saturated chain at the *sn*-1 position and a range of chains with 0−6 double bonds at the *sn*-2 position ($S_{CD} = 0.35$) (*12*). Whether the sterol aligns perpendicular to the bilayer normal at the interface between monolayers (Figure 4B) or parallel to the bilayer and inverted (Figure 4C) cannot be ascertained from the spectral shape. The spectrum is a powder pattern characteristic of rapid rotation

about an axis of indeterminate direction. Assuming an upright disposition, a tilt angle of $\alpha_0 = 22 \pm 1°$ relative to the bilayer normal was calculated from the quadrupolar splitting (*12*). This angle could equally apply to a most probable orientation relative to an axis parallel to the plane of the membrane for a steroid molecule lying between leaflets or relative to the bilayer normal for an inverted steroid molecule.

In conclusion, we have presented an extraordinary result showing that the hydroxyl end of [2,2,3,4,4,6-$^2H_6$] cholesterol lies at the center of 20:4−20:4 PC membranes. This profound change in orientation of the sterol molecule in bilayers made up entirely of polyunsaturated acyl chains represents a dramatic manifestation of the unique properties of PUFA. The physiological implications, at this point, are still to be considered. Although rare in general, dipolyunsaturated phospholipids are abundant in certain specialized membranes such as in the retina (*36*). Further experiments on cholesterol analogues with additional labels are planned to exactly orient the cholesterol molecule within the bilayer.

ACKNOWLEDGMENT

We thank Michael R. Brzustowicz for his contribution to the genesis of this investigation. T.A.H. and J.K. acknowledge the financial support received from The Advanced Foods and Materials Network (Networks of Centres of Excellence, Canada).

REFERENCES

1. Stillwell, W., and Wassall, S. R. (2003) Docosahexaenoic acid: Membrane properties of a unique fatty acid, *Chem. Phys. Lipids 126*, 1−27.
2. Wassall, S. R., Brzustowicz, M. R., Shaikh, S. R., Cherezov, V., Caffery, M., and Stillwell, W. (2004) Order from disorder, corralling cholesterol with chaotic lipids. The role of polyunsaturated lipids in membrane raft formation, *Chem. Phys. Lipids 132*, 79−88.
3. Huster, D., Arnold, K., and Gawrisch, K. (1998) Influence of docosahexaenoic acid and cholesterol on lateral lipid organization in phospholipid mixtures, *Biochemistry 37*, 17299−17308.
4. Mitchell, D. C., and Litman, B. J. (1998) Molecular order and dynamics in bilayers consisting of highly polyunsaturated phospholipids, *Biophys. J. 74*, 879−891.
5. Finegold, L. (1993) *Cholesterol in Membrane Models*, CRC Press, Boca Raton, FL.
6. Vist, M. R., and Davis, J. H.(1990) Phase equilibria of cholesterol/dipalmitoylphosphatidylcholine mixtures: ^{2}H nuclear magnetic resonance and differential scanning calorimetry, *Biochemistry 29*, 451−464.
7. Huang, J., Buboltz, J. T., and Feigenson, G. W. (1999) Maximum solubility of cholesterol in phosphatidylcholine and phosphatidylethanolamine bilayers, *Biochim. Biophys. Acta 1417*, 89−100.
8. Léonard, A., Escriv, C., Laguerre, M., Pebay-Peyroula, E., Néri, W., Pott, T., Katsaras, J., and Dufourc, E. J. (2001) Location of cholesterol in DMPC membranes. A comparative study by neutron diffraction and molecular mechanics simulation, *Langmuir 17*, 2019−2030.
9. Marsan, M. P., Muller, L., Ramos, C., Rodriguez, F., Dufourc, E. J., Czaplicki, J., and Milon, A. (1999) Cholesterol orientation and dynamics in dimyristoylphosphatidylcholine bilayers: A solid-state deuterium NMR analysis, *Biophys. J. 76*, 351−359.
10. Thewalt, J. L., and Bloom, M. (1992) Phosphatidylcholine: Cholesterol phase diagrams, *Biophys. J. 63*, 1176−1181.
11. Worcester, D. L., and Franks, N. P. (1976) Structural analysis of hydrated egg lecithin and cholesterol bilayers, *J. Mol. Biol. 100*, 359−378.
12. Brzustowicz, M. R., Stillwell, W., and Wassall, S. R. (1999) Molecular organization of cholesterol in polyunsaturated phospholipid membranes: A solid state ^{2}H NMR investigation, *FEBS Lett. 451*, 197−202.
13. Niu, S. L., and Litman, B. J. (2002) Determination of membrane cholesterol partition coefficient using a lipid vesicle−cyclodextrin binary system: Effect of phospholipid acyl chain unsaturation and headgroup composition, *Biophys. J. 83*, 3408−3415.
14. Pitman, M. C., Suits, F., MacKerell, A. D., Jr., and Feller, S. E. (2004) Molecular-level organization of saturated and polyunsaturated fatty acids in a phosphatidylcholine bilayer containing cholesterol, *Biochemistry 43*, 15318−15328.
15. Brzustowicz, M. R., Cherezov, V., Caffrey, M., Stillwell, W., and Wassall, S. R. (2002) Molecular organization of cholesterol in polyunsaturated membranes: Microdomain formation, *Biophys. J. 82*, 285−298.
16. Brzustowicz, M. R., Cherezov, V., Zerouga, M., Caffrey, M., Stillwell, W., and Wassall, S. R. (2002) Controlling membrane cholesterol content. A role for polyunsaturated (docosahexaenoate) phospholipids, *Biochemistry 41*, 12509−12519.
17. Feller, S. E., Gawrisch, K., and MacKerell, A. D., Jr. (2002) Polyunsaturated fatty acids in lipid bilayers: Intrinsic and environmental contributions to their unique physical properties, *J. Am. Chem. Soc. 124*, 318−326.
18. Zaccaï, G., Blasie, J. K., and Schoenborn, B. P. (1975) Neutron diffraction studies on the location of water in lecithin bilayer model membranes, *Proc. Natl. Acad. Sci. U.S.A. 72*, 376−380.
19. Büldt, G., Gally, H. U., Seelig, J., and Zaccai, G. (1979) Neutron diffraction studies on phosphatidylcholine model membranes, *J. Mol. Biol. 134*, 673−691.
20. Zaccaï, G., Büldt, G., Seelig, A., and Seelig, J. (1979) Neutron diffraction studies on phosphatidylcholine model membranes, *J. Mol. Biol. 134*, 693−706.
21. Wiener, M. C., and White, S. H. (1991) Fluid bilayer structure determination by the combined use of X-ray and neutron diffraction. 1. Fluid bilayer models and the limits of resolution, *Biophys. J. 59*, 162−173.
22. Wiener, M. C., and White, S. H. (1991) Fluid bilayer structure determination by the combined use of X-ray and neutron diffraction. 2. "Composition-space" refinement method, *Biophys. J. 59*, 174−185.
23. Bradshaw, J. P., Bushby, R. J., Giles, C. C. D., and Saunders, M. R. (1999) Orientation of the headgroup of phosphatidylinositol in a model biomembrane as determined by neutron diffraction, *Biochemistry 38*, 8393−8401.
24. Franks, N. P., and Lieb, W. R. (1979) The structure of lipd bilayers and the effects of general anaesthetics, *J. Mol. Biol. 133*, 469−500.
25. Hauss, T., Dante, S., Dencher, N. A., and Haines, T. H. (2002) Squalane is in the midplane of the lipid bilayer: Implications for its function as a proton permeability barrier, *Biochim. Biophys. Acta 1556*, 149−154.
26. Bradshaw, J. P., Darkes, M. J. M., Harroun, T. A., Katsaras, J., and Epand, R. M. (2000) Oblique membrane insertion of viral fusion peptide probed by neutron diffraction, *Biochemistry 39*, 6581−6585.
27. Dante, S., Hauss, T., and Dencher, N. A. (2002) β-Amyloid 25 to 35 is intercalated in anionic and zwitterionic lipid membranes to different extents, *Biophys. J. 83*, 2610−2616.
28. Gordeliy, V. I., and Chernov, N. I. (1997) Accuracy of determination of position and width of molecular groups in biological and lipid membranes via neutron diffraction, *Acta Crystallogr., Sect. D: Biol. Crystallogr. 53*, 377−384.
29. Katsaras, J., Jeffrey, K. R., Yang, D. S.-C., and Epand, R. M. (1993) Direct evidence for the partial dehydration of phosphatidylethanolamine bilayers on approaching the hexagonal phase, *Biochemistry 32*, 10700−10707.
30. Katsaras, J., and Stinson, R. H. (1990) High-resolution electron density profiles reveal influence of fatty acids on bilayer structure, *Biophys. J. 57*, 649−655.
31. Katsaras, J. (1995) Structure of the subgel ($L_{c'}$) and gel ($L_{\beta'}$) phases of oriented dipalmitoylphosphatidylcholine multibilayers, *J. Phys. Chem. 99*, 4141−4147.
32. Rajamoorthi, K., Petrache, H. I., McIntosh, T. J., and Brown, M. F. (2005) Packing and viscoelasticity of polyunsaturated ω-3 and ω-6 lipid bilayers as seen by ^{2}H NMR and X-ray diffraction, *J. Am. Chem. Soc. 27*, 1576−1588.
33. Eldho, N. V., Feller, S. E., Tristram-Nagle, S., Polozov, I. V., and Gawrisch, K. (2003) Polyunsaturated docosahexaenoic vs docosapentaenoic acid−Differences in lipid matrix properties from the loss of one double bond, *J. Am. Chem. Soc. 125*, 6409−6421.

34. Murari, R., Murari, M. P., and Baumann, W. J. (1986) Sterol orientations in phosphatidylcholine liposomes as determined by deuterium NMR, *Biochemistry 25*, 1062−1067.
35. Smaby, J. M., Momsen, M. M., Brockman, H. L., and Brown, R. E. (1997) Phosphatidylcholine acyl unsaturation modulates the decrease in interfacial elasticity induced by cholesterol, *Biophys. J. 73*, 1492−1505.
36. Aveldano, M. I. (1989) Dipolyunsaturated species of retina phospholipids and their fatty acids, *Colloq. INSERM 195*, 87−96.
37. Kraulis, P. J. (1991) MOLSCRIPT: A program to produce both detailed and schematic plots of protein structures, *J. Appl. Crystallogr. 24*, 946−950.

BI0520840